Appl Water Sci (2013) 3:741–751
DOI 10.1007/s13201-013-0122-1

ORIGINAL ARTICLE

A study on the defluoridation in water by using natural soil

S. Chidambaram · S. Manikandan · AL. Ramanathan · M. V. Prasanna · C. Thivya · U. Karmegam · R. Thilagavathi · K. Rajkumar

Received: 11 April 2013 / Accepted: 9 July 2013 / Published online: 25 July 2013

Abstract Removal of excess fluoride (F^-) from the water has been attempted by several authors by using different materials both natural and artificial. The main aim of this paper was to attempt the fluoride removal by using the locally available red soil adopting column method. The red soil was mixed in different proportion with sand in order to increase the porosity and permeability property of the medium. It was optimized for 4:1 ratio of red soil to sand and it was used for the following experiment. The experiment was conducted in 11 batches for a period of about 9,213 min. Fresh standard solution of F was used in each batch, prepared from Orion 1,000 ppm solution. The samples were collected and analyzed for pH, EC (Electrical Conductivity) and HCO_3. Rate of flow of water and efficiency of adsorption were calculated and compared with the fluoride removal capacities of the medium. The medium used for the fluoride removal was subjected to FTIR analysis before and after the experiment. The variation of IR spectrum before and after treatment signifies the changes in the OH bonding between Al and Fe ions present in the soil. The variation in pH decreased during the course of defluoridation. Higher F removal was noted when flow rate was lesser. An attempt on the regeneration of the fluoride adsorbed soil was also made and found to be effective.

Keywords Defluoridation · Adsorption capacity · FTIR spectrum · Removal efficiency · Natural soil

S. Chidambaram · S. Manikandan · C. Thivya · U. Karmegam · R. Thilagavathi
Department of Earth Sciences, Annamalai University, Annamalai Nagar 608 002, India

AL. Ramanathan · K. Rajkumar
School of Environmental Sciences, Jawaharlal Nehru University, New Delhi 110067, India

M. V. Prasanna (✉)
Department of Applied Geology, School of Engineering and Science, Curtin University, CDT 250, 98009 Miri, Sarawak, Malaysia
e-mail: geoprasanna@gmail.com

Introduction

Excess of fluoride in groundwater has become a threat in recent days due to the lesser availability of potable groundwater resource. There are different methods of defluoridation proposed by different authors, like ion exchange, precipitation and adsorption. Among these methods, adsorption is a widely used method for defluoridation of water because of its easy method of operation and cost effectiveness. Some of the adsorption materials broadly used for defluoridation are; physico-chemically treated sand (Togarepi et al. 2012), microwave assisted activated carbon (Dutta et al. 2012), aluminum sulfate treatment (Malay and Salim 2011), pumice (Malakootian et al. 2011) and raw Bauxite (Sajidu et al. 2012). An extensive survey on the removal of excess fluoride in water shows that different techniques has been attempted by several authors, using natural and synthetic material (Table 1). This review of the literature shows that the study of fluoride removal by natural materials/soil is less. One such attempt was made (Chidambaram 2000; Chidambaram et al. 2003) for removal of fluoride in groundwater by using natural materials and showed that, untreated charcoal seems (Table 2) to have lesser effect on the concentrations of fluoride with time and it adsorbs only 0.5–1 mgl^{-1} of fluoride. The brick and fly-ash show typically a sudden removal of fluoride to 6.6 and 5.6 mgl^{-1} respectively. >50 % reduction of concentration takes place within 30 min. Red

Table 1 The removal of excess fluoride in water has been attempted by several authors

S·No	Methods	Authors (Year)
1	Adsorption of Fluoride by soils and minerals	Bower and Hatcher (1967)
2	Optimization of fluoride removal from brackish water by electrodialysis	Amor et al. (1998)
3	Fluoride removal from waters by Donnan dialysis	Hichour et al. (2000)
4	Fluoride removal Corn brackish water by electro dialysis	Amof et al. (2001)
5	Defluoridation of Sahara water by small plant electrocoagulation using bipolar aluminium electrodes	Mameri et al. (2001)
6	Integrated biological and physiochemical treatment process for nitrate and fluoride removal	Mekonen et al. (2001)
7	Defluoridation of groundwater by a hybrid process combining adsorption and Donnan dialysis	Garmes et al. (2002)
8	Deflouridation of water using amended clay	Agarwal et al. (2003)
9	Effects of co-existing anions on fluoride removal in electrocoagulation (EC) process using aluminum electrodes	Hu et al. (2003)
10	Appropriate deflouridation technology for use in flourotic areas in Tanzania	Mjengera and Mkongo (2003)
12	Defluoridation of Moroccan ground water by electrodialysis: continuous operation	Tahaikt et al. (2004)
13	Effects of the molar ratio of hydroxide and fluoride to Al (III) on fluoride removal by coagulation and electrocoagulation	Hu et al. (2005)
14	Development of Defluoridation Technology for its Easy Adaptation in Rural Areas	Singh et al. (2004)
15	Removal of fluoride from drinking water by adsorption onto alum-impregnated activated alumina	Tripathy et al. (2006)
16	Removal of troublesome anions from water by means of Donnan dialysis	Wisniewski et al. (2005)
17	Defluoridation of groundwater using brick powder as an adsorbent	Yadav et al. (2006)
18	Defluoridation of drinking water using activated titanium rich bauxite	Das et al. (2005)
19	Defluoridation of Moroccan groundwater by electrodialysis: continuous operation	Tahaikt et al. (2006)
20	Fluoride in drinking water and its removal	Meenakshi and Maheshwari (2006)
21	Investigations on activated alumina based domestic defluoridation units	Chauhan et al. (2007)
22	Defluoridation of drinking water using chitin, chitosan and lanthanum-modified chitosan	Kamble et al. (2007)
23	Defluoridation of drinking water by calcined MgAl-CO_3 layered double hydroxides	Lv et al. (2007)
24	Fluoride distribution in electrocoagulation defluoridation process	Zhu et al. (2007)
25	Insights into isotherm making in the sorptive removal of fluoride from drinking water	Ayoob and Gupta (2008)
26	Investigations on the kinetics and mechanisms of sorptive removal of fluoride from water using alumina cement granules	Ayoob et al. (2008)
27	Removal of excess fluoride from water using waste residue from alum manufacturing process	Nigussie et al. (2007)
28	Economic evaluation of fluoride removal by electrodialysis	Lahnida et al. (2008)
29	Comparison of the performances of three commercial membranes in fluoride removal by nanofiltration. Continuous operations	Tahaikta et al. (2008)
30	Defluoridation chemistry of synthetic hydroxyl apatite at nano scale: Equilibrium and kinetic studies	Sairam Sundaram et al. (2008a, b)
31	Defluoridation of wastewaters using waste carbon slurry	Gupta et al. (2007)
32	Sorptive response profile of an adsorbent in the defluoridation of drinking water	Ayoob and Gupta (2007)
33	Uptake of fluoride by nano- hydroxyapatite/chitosan, a bioinorganic composite	Sairam Sundaram et al. (2008a, b)
34	Role of metal ion incorporation in ion exchange resin on the selectivity of fluoride	Viswanathan and Meenakshi (2009b)
35	Electrodialytic removal of fluoride from water: Effects of process parameters and accompanying anions	Erdem Ergun et al. (2008)
36	Removal of fluoride from aqueous solution using protonated chitosan beads	Viswanathan et al. (2009a)
37	Development of multifunctional chitosan beads for fluoride removal	Viswanathan et al. (2009c)
38	Sorption behaviour of fluoride on carboxylated cross-linked chitosan beads	Viswanathan et al. (2009b)
39	Enhanced fluoride sorption using La(III) incorporated carboxylated chitosan beads	Viswanathan and Meenakshi (2008)
40	Treatment of fluoride containing drinking water by electrocoagulation using monopolar and bipolar electrode connections	Ghosh et al. (2008)
41	Defluoridation from aqueous solutions by granular ferric hydroxide (GFH)	Kumar et al. (2009)
42	Defluoridation of water using neodymium-modified chitosan	Yao et al. (2008)

Table 1 continued

S·No	Methods	Authors (Year)
43	Size-dependent defluoridation properties of synthetic hydroxyapatite	Gao et al. (2008)
44	Adsorption of fluoride by hydrous iron(III)–tin(IV) bimetal mixed oxide from the aqueous solutions	Biswas et al. (2009)
45	Bleaching powder: A versatile adsorbent for the removal of fluoride from aqueous solution	Kagne et al. (2009)
46	Characterization and Defluoridation studies of activated dolichos lab lab carbon	Rao et al. (2009)
47	Defluoridation of water using as-synthesized Zn/Al/Cl anionic clay adsorbent: Equilibrium and regeneration studies	Mandal and Mayadevi (2009)
48	Fluoride removal from water using activated and MnO_2-coated Tamarind Fruit (Tamarindus indica) shell: Batch and column studies	Sivasankara et al. (2010)
49	Comments on "Defluoridation of water using neodymium-modified chitosan"	Ho (2009)
50	Removal of fluoride from water using aluminium containing compounds	Karthikeyan and Elango (2009)
51	Performance evaluation of alumina cement granules in removing fluoride from natural and synthetic waters	Ayoob and Gupta (2009)
52	Fluoride sorption using organic–inorganic hybrid type ion exchangers	Sairam Sundaram and Meenakshi (2009)
53	Study on the fluoride adsorption of various apatite materials in aqueous solution	Gao et al. (2009)
54	Defluoridation of drinking water by electrocoagulation/electroflotation in a stirred tank reactor with a comparative performance to an external-loop airlift reactor	Essadki et al. (2009)
55	Characteristics and defluoridation performance of granular activated carbons coated with manganese oxides	Yue Ma et al. (2009)
56	Removal and adsorption characteristics of polyvinyl alcohol from aqueous solutions using electrocoagulation	Chou (2010)
57	Adsorption behavior of fluoride ions using a titanium hydroxide-derived adsorbent	Wajima et al. (2009)
58	Fluoride adsorption onto granular ferric hydroxide: Effects of ionic strength, pH, surface loading, and major co-existing anions	Tang et al. (2009)
59	Removal of fluoride from aqueous environment by modified Amberlite resin	Solangi et al. (2009)
60	Fluoride removal using lanthanum incorporated chitosan beads	Bansiwal et al. (2009)
61	Study on the fluoride adsorption of various apatite materials in aqueous solution	Gao et al. (2009)
62	Review of fluoride removal from drinking water	Mohapatra et al. (2009)
63	Conducting polymer/alumina composites as viable adsorbents for the removal of fluoride ions from aqueous solution	Karthikeyan et al. (2009)
64	Removal of fluoride ions from aqueous solution by waste mud	Kemer et al. (2009)
65	Synthesis of Zr(IV) entrapped chitosan polymeric matrix for selective fluoride sorption	Viswanathan and Meenakshi (2009a)
66	Economical evaluation of the fluoride removal by nanofiltration	Elazhar et al. (2009)
67	Copper oxide incorporated mesoporous alumina for defluoridation of drinking water	Bansiwal et al. (2010)
68	Chitosan based mesoporous Ti–Al binary metal oxide supported beads for defluoridation of water	Thakrea et al. (2010)
69	Fluoride removal for underground brackish water by adsorption on the natural chitosan and by electrodialysis.	Annouar et al. (2007)
70	Defluoridation of brackish northern Sahara groundwater—activity product calculations in order to optimize pretreatment before reverse osmosis	Nicolas et al. (2010)

soil absorbs 9 mgl^{-1} of fluoride immediately after 15 min. After 30 min the fluoride decreases from 0.09 mgl^{-1} and keeps on reducing with time up to 0.035 mgl^{-1} in 90 min to 0.039 mgl^{-1} at 120 min. In serpentine the fluoride removal was found to be maximum from 0 to 15 min, i.e. 3.7 mgl^{-1}: later the defluoridation capacity decreases to 5.8 mgl^{-1} at 120 min. But the defluoridation capacity is less when compared to red soil. The study reveals that among these five materials used for defluoridation red soil has a good defluoridation capacity followed by brick, serpentine, fly-ash and charcoal. Near equilibrium is attained after about 30 min of the experiment in red soil and brick (Table 2). Maximum defluoridation occurs immediately after the experiment has started in almost all the materials used except for lesser impact on charcoal. The molality of fluoride removed per gram is higher in red soil when

Table 2 Fluoride in time intervals (all the values are in mgl^{-1})

Time (min)	Red soil	Charcoal	Fly-ash	Brick	Serpentine
15	0.64	9.05	3.4	4.7	3.7
30	0.09	9.05	3.7	4	4.1
60	0.06	9.1	4.7	3.7	4.6
90	0.035	9.05	6	4	4.8
120	0.029	9	7.1	3.9	5.8

Table 3 Assignment of bands observed in FTIR spectrum

Band Observed/cm^{-1}	Assignment
3.698	O–H Stretch of inner surface
	Al–O–H groups between kaolinite layers
3.627	O–H stretch of the inner
	Al–O–H between siloxane and alumina sheet within layers
1.117	Si–O stretch
1.073	Si–O stretch
1.038	Si–O-Si stretch
1.013	Si–O–Al stretch
795	Si–O stretch
695	Si–O–Al stretch
586	Al–O stretch

compared to the other materials. Red lateritic soil has the highest fluoride removal capacity because it has oxide of aluminium and iron as its major components. In general aluminum compounds are found to be good fluoride removers because of reaction between Al^{-} and F^{-} molecules (Chidambaram et al. 2003). Hence, both Al^{-} and Fe^{-} in red soil are found to be a good removers of fluoride. The column study thus reveals that the quantity of materials used were according to their effective fluoride removal capacity. But this study lacks detailed monitoring of data over a periodic time interval, where sequential changes can occur rapidly; further, the materials were not examined/studied before and after the treatment. Keeping these factors in mind, red soil which is an effective fluoride remover was used in this study to understand the fluoride removal capacity over time. They are also studied for their change in their bonding nature before and after the treatment. Further an attempt was also made to understand their regeneration property/capacity after this experiment.

Materials and methods

A column was set up for the study by using mixture of red soil and sand with a ratio by weight of 4:1. It is noted that the red soil is fine grained substance with clay size particles and, with good ion exchange capacity but lesser permeability, hence it was mixed with sand to increase the permeability. The removal rate of fluoride was tested using 250 gm of mixture soil (200 g of red soil and 50 g of sand). The fluoride concentration in the samples was measured by using an Orion, model 2100 expandable ion analyzer EA 940 and the fluoride ion selective electrode BN 9609 (Orion, Thermo Fisher Scientific, USA). The standard solution of 10 mg/l fluoride was prepared from 100 mgl^{-1} standard (Thermo Orion) by using DDW (Doubled Distilled Water). The samples were collected at definite intervals. Eleven different Batch experiments were conducted by passing Fluoride standard of 10 mgl^{-1}. 10 ml of sample was collected after the treatment and analyzed. A total of about 62 samples were collected in different batches during the entire experimental period. Out of these samples collected, different parameters were observed along with F concentration. Rate of flow of water through the column, their variation in pH, Percentage of fluoride adsorption, adsorption capacity, bicarbonate concentration and EC were also observed. pH and EC were analyzed by ion sensitive electrodes, HCO_3 was estimated by titrimetry method using standard procedures (APHA 1998).

The adsorption capacity was calculated by using the formula,

$$q_e(\text{mmol/g}) = (\text{Co} - \text{Ce}) \times V/W \times 1{,}000$$

Ce is equilibrium adsorbate (fluoride) concentration (mmol/l). Co is initial adsorbate (fluoride) concentration (mmol/l). q_e amount of fluoride adsorbed per unit gram of the adsorbant at equilibrium (mmol/g). V is volume of solution (l). W is weight of adsorbant (g).

Results and discussion

FTIR

Fourier Transform Infrared (FTIR) spectroscopy is an established experimental technique for determining qualitative mineral identification and is currently being developed for quantitative mineralogy. The majority of the natural earth materials are silicates, carbonates, phosphates, etc. The elementary building unit of the silicate minerals is the 4 SiO tetrahedron having a net–4 charge. The interlinking of the 4 SiO tetrahedra results in formation of various polymers (Makreski et al. 2005). The structural classification of the silicate minerals is in fact based on the extent of sharing of oxygen anions between the adjacent tetrahedra. It makes the silicates the largest and the most complicated class of minerals. An important associate ion of the silicate mineral group is OH.

Fe–Al and OH bondings

The intensity and especially the frequency of the IR band in the *v* (OH) region could serve as a tool for reliable estimation of the Fe and/or Al content. Fe and Al are the dominant ions in the red soil; the strength of O–H bond slightly differs when different cations are coordinated to the hydroxyl groups as it is depicted in the FTIR spectrum (Table 3). A simple harmonic model of different M^{3+}–O oscillators (M = Fe and/or Al in red soil) may result in frequency shifting of the band in the spectrum (Makreski et al. 2007). The effect of Fe substituting for Al at the non-OH coordinated M1 and especially M3 octahedral site causes an increase in the bond strength at the O_4 atom ([M2] Al–O_{10}–H···O_4–[M1] Al [M1] Al [M3] Fe) for Fe it is principally due to the difference in the electronegativity with respect to Al (Della Ventura et al. 1996). Since the maximum of the OH stretching vibration in our IR spectrum is observed at 3,450 cm^{-1}. *v*(OH) vibrations in the OH bearing minerals are generally observed in the 3,600–3,400 cm^{-1} region, the band at 3,627 cm^{-1} probably arise from FeOH stretching, whereas the strongest band at 3,450 cm^{-1} has OH and perhaps somewhat 2HO stretching mode character.

Sorosilicate in FTIR spectra

The presence of the bands in many sorosilicate spectra studied (Denning et al. 1972; Lazarev 1972) at frequencies 1,170–1,080 cm^{-1} much above those from nesosilicates (Makreski et al. 2005) implies that these bands could be assigned as *v* as (Si–O_b–Si) modes (O_b denotes bridging oxygen). Therefore, the origin of the band at 1,088 cm^{-1} is not questionable and should be attributed to the mentioned Si–O vibration. According to Wang et al. (1994) the symmetric stretching vibration of Si–O_b–Si type should be expected in the 750–450 cm^{-1} region, this mode was prescribed to the strong band at 695 cm^{-1}.

The assignment of the bands in the 700–500 cm^{-1} region was much more complicated because, in addition to the Si–O–Si deformation modes, this region is also typical for the OH vibrational modes. It causes the bands in this region to be overlapped and even partly coupled because the OH modes were expected to appear in wide region. Taking these considerations into account, the weak bands at 795, 695 and 586 cm^{-1} were assigned as predominantly bending Si–O–Si vibrations whereas the strong band beyond 586 cm^{-1} (absent in the studied non-hydroxide pyroxenes) probably is a result of out-of-plane bending OH vibrations.

Variation in the FTIR Spectra of Muscovite, Phlogophite, Actinite and Aragonite minerals were identified by FTIR. The Phlogophite observed very strong band at 465.31 cm^{-1} (Si–O–Si) vibration. The Quartz observed strong band at 463.57 $cm^{-1.}$ The Muscovite observed very strong band at 1038.25 cm^{-1} in the Si–O vibration. The Montmorillonite is observed at 1,629 cm^{-1} in the H–O–H bending vibration. The Kaolinite is observed Lattice band at 3627.40 $cm^{-1}$and Al–O–H stretching at 3,620–3,692 cm^{-1}. The maxima at 3,704 cm^{-1} and 3,627 cm^{-1} represent the OH stretching with the following cation combinations $Mg^{2+}Mg^{2+}Mg^{2+}$, $Mg^{2+}Mg^{2+}Fe^{2+}$, $Mg^{2+}Fe^{2+}Fe^{2+}$ and $Fe^{2+}Fe^{2+}Fe^{2+}$. The substantial broadening of the series of bonds by substitution of Fe^{3+} by Al^{3+} in other amphiboles on, the smaller six-fold coordinated Fe^{3+} cations which gets generally concentrated in M2 sites studied (Wilkens 1970; Hawthorne 1983; Skogby and Annersten 1985). Therefore, the lowest frequency OH stretching peaks at 3,523 and 3,450 cm^{-1} are prescribed to the $Fe^{2+}Fe^{2+}Fe^{3+}$ and $Fe^{2+}Fe^{3+}Fe^{3+}$ cation combinations, respectively, being in accordance with the literature data for Actinolite mineral (Mustard 1992). The *v* (OH) region has shown that studied mineral contains both Mg^{2+} and Fe^{2+} cations.

Sediments which are Mg^{2+} rich and poor in Fe^{2+} show absorptions at 620 and 586 cm^{-1} that are not found in others specimens. According to Stubican and Roy (1961a, b) the strong absorption is observed between 620 and 692 cm^{-1} assigned to Si–O vibration the one near 550 cm^{-1} to Si–O–Al ^{VI} vibration, the one near 760 cm^{-1} to Si–O vibration and another near 830 cm^{-1} to Si–O–Al vibration. It is also reported that an absorption due to H–O–Fe would appear near 812 cm^{-1} which is absent in the spectra before and after treatment and one represented by Si–O–Fe ^{VI} vibration would be found near 495 cm^{-1} (Stubican and Roy 1961b).

It is due to the fact that the pyroxene structure is built by the complex chains of 4 SiO anions whereas the 4 SiO building blocks in the nesosilicates are isolated. Such structural difference perturbs the degeneracy of the *v*2, *v*3 and *v*4 modes in the pyroxene infrared spectra (Sterns 1974) causing the appearance of larger number of IR bands as a result of the different bonding between the terminal (Ot) and bridging (Ob) oxygen to the Si atoms. In this context, the highest wave number peaks were assigned as the Si–Ot rather than Si–Ob modes. It is due to their greater force constants compared to the Si–Ob modes, because the Si–Ob motions are additionally shared between the adjacent tetrahedra. On the other hand, the wave numbers of the bands in this region are nearly constant suggesting that chain vibrations are not particularly sensitive to the population of the cation sites by Rutstein and White (1971). It means that the observed bands in the 1,100-850 cm^{-1} regions are, to great extent, due to pure *v* (O–Si–O) and *v* (Si–O–Si) vibrations.

For experimental quantitative and to understand changes in the adsorbent (if any) due to fluoride sorption, FTIR

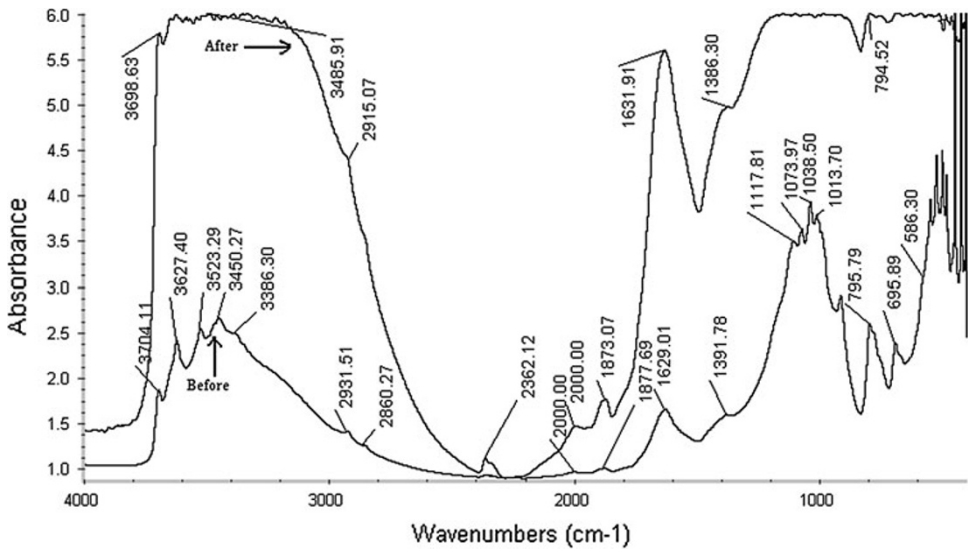

Fig. 1 FTIR spectrum of the mixture before and after the experiment

analysis were done before and after adsorption. As shown in Fig. 1, the FTIR spectrum of the samples presents significant spectroscopic change due to fluoride sorption. The broad band corresponding to 3,450 cm^{-1} (range of 3,698–3,380 cm^{-1}) represents OH stretching vibrations that at 1,391 cm^{-1} to Al H stretching and 1,013 cm^{-1} represents the characteristic stretching bands of Si–O–Al. The band at 586 cm^{-1} may be ascribed to the stretching of Al OH. On closer examination, it has been observed that the intensity of many of the peaks shows variations after fluoride sorption. Chukin and Malevich (1977) demonstrated that the treatment of SiO_2 sample with fluoride results in a decrease in the intensity of the $(OH)^-$ band at 3,704 cm^{-1} or its complete disappearance due to fluoride uptake. This is readily explained, since it is known that $(OH)^-$ and F^- ions have closely similar dimensions and can isomorphously replace each other. So, to ascertain whether such an exchange reaction is taking place in the fluoride sorption onto absorbant, the ratio of peak heights of the unbounded surface $(OH)^-$ band at 3,386 cm^{-1} to that at 3,700 cm^{-1} are compared before and after adsorption. Before adsorption, in the virgin adsorbent this peak height was 2.56, but after fluoride sorption, it is found to be 6 in the fluoride adsorbent. This shows that the OH^- band at 3,704 cm^{-1} is decreasing due to fluoride sorption, confirming the exchange of OH ions, enhancing fluoride removal. In the similar way, the peak height of $(OH)^-$ band at 3,627 cm^{-1} to that of Al OH band at 586 cm^{-1} is also compared to infer the changes before and after treatment.

Effect of pH in fluoride removal

To understand the fluoride sorption behavior under different pH values sorption was monitored, under (Kamble et al. 2007; Sarkar et al. 2006) the neutral, protonated and deprotonated sites. Behavior of the adsorbent towards fluoride removal mainly depends on the initial solution pH. The effect of pH on fluoride removal performance of the adsorbent was studied over a wide pH range of 3–11 by different authors (Togarepi et al. 2012; Dutta et al. 2012; Malakootian et al. 2011). For the same system, protonation and subsequent F^- sorption via ligand exchange may also explain F^- removal at pH <6.5, in accordance with following equations:

$$M - OH + H^+ \rightarrow M - OH_2^+ \quad \text{(R1)}$$

$$M - OH_2^+ + F^- \rightarrow M^+ - F^- + H_2O \quad \text{(R2)}$$

Where, M represents metal ions like Al^{3+}, Fe^{3+}. The supported iron and aluminum oxides form the aqua complex with water and form the surface charges through amphoteric dissociation. At acidic pH, more positively charged surface sites developed which attract the negatively charged fluoride ions by electrostatic attraction resulting in the enhanced fluoride removal at acidic pH (Denning et al. 1972; Lazarev 1972; Wang et al. 1994). Reactions (R1) and (R2) hold true for fluoride adsorption at acidic medium.

$$M - OH + F^- \rightarrow M - F + OH^- \quad \text{(R3)}$$

Where, M represents metal ions like Al^{3+}, Fe^{3+}. Reaction (R3) represents the ligand-exchange interaction between fluoride and hydroxyl ions at neutral pH. It is known that at pH <7, free bases are feebly ionized and reaction (3) does not proceed rapidly to the right as compared to the reactions (1) and (2) (Ramos et al. 1999). The pH increase of initial solution in the experiment is near to 10 which have no significance influence on fluoride removal efficiency. Further increase in pH above 10 drastically reduces the fluoride removal efficiency by 52 %, which may be due to the competition between hydroxide and fluoride ions for active sites in this

Table 4 The maximum, minimum and average values of rate of flow, pH, adsorption, HCO_3 and EC

	Rate of flow (mls^{-1})	PH	Adsorption (%)	Adsorption capacity	HCO_3 (mg/L)	EC (μs/cm)
Maximum	0.83	95.0	96.00	0.0038	707.60	4354.00
Minimum	0.02	6.63	0.00	0.0000	24.40	291.00
Average	0.22	7.69	86.45	0.0025	182.80	723.52

Table 5 Correlation analysis for the parameters observed during the experiment

	Rate of flow	pH	Removal efficiency	Adsorption capacity	HCO_3	EC
Rate of flow	1.00					
pH	0.58	1.00				
Removal efficiency	0.03	−0.17	1.00			
Adsorption capacity	−0.22	−0.53	0.59	1.00		
HCO_3	−0.50	−0.57	−0.04	0.30	1.00	
EC	0.22	0.03	0.04	0.42	0.04	1.00

pH range. The decrease in adsorption at higher pH value (pH>10) may also be possible due to abundance of $(OH)^-$ ions which leads to increased hindrance to diffusion of fluoride ions by Stubican and Roy (1961b). Exchangeable Ca^{2+} present in soil at near neutral pH has been reported by some workers (Mustard 1992; Stubican and Roy 1961a). In all the cases, decreased F^- removal at high pH may be due to the existence of an hydroxyl envelope on solid particles causing negative surface charge, which would effectively repel F^- from the sorption sites and simultaneously compete with them (Rutstein and White 1971). At the later stage of the experiment the pH of the treated water shows increase of (H^+) concentration by decrease in pH values $M\text{-}OH_2 + F^- \rightarrow M\text{-}F^- + H^+ + (OH)^-$. At higher pH value, a slight decrease in fluoride removal was observed. Similar observation in the reduction of fluoride removal capacity at alkaline pH ranges may be attributed to the competition from the negatively charged $(OH)^-$ ions by Ghorai and Pant (2005). A sharp decrease in fluoride removal was noted (Denning et al. 1972) and they attributed it due to the formation of the weakly ionized HF (pKa = 3.2) at low pH values and due to the competitiveness of the $(OH)^-$ and F^- ions in the bulk, at high pH values.

EC and HCO_3 variations

The variation in the batches indicates that the electrical conductivity generally decreases after the batch reactions. It shows increasing trend in batch 8 and 11. This may be due to the regeneration process during the flow of water and saturation of the available exchange sites. Though bicarbonate concentration shows fluctuation but generally exhibit a decreasing trend except in batch 8, where both the HCO_3 and EC shows increasing trend.

The study shows that rate of flow ranges maximum from 0.02 to 0.83 mls^{-1} with an average of 0.22 mls^{-1}. The pH shows maximum from 9.50 to minimum 6.63 with an average of 7.69, the percent of adsorption shows maximum from 96 to minimum BDL (Below Detection Limit) with an average of 86.45 (Table 4). Adsorption capacity ranges with a maximum of 0.0038 and a minimum BDL with an average of 0.0025, the HCO_3 ranges with a maximum from 707.60 mgl^{-1} to a minimum of 24.40 mgl^{-1} with an average of 182.80 mgl^{-1} and the EC ranges with maximum from 4354 μs/cm to a minimum of 291 μs/cm with an average of 723.52 μs/cm. The correlation analyses of the parameters were carried out and these parameters show that the rate of flow of water has positive correlation to pH and negative to HCO_3, pH has negative correlation to all other parameters, with strong negative correlation to fluoride adsorption capacity and HCO_3 (Table 5). This indicates that the efficiency of fluoride removal increases when HCO_3 concentration decreases. The efficiency of fluoride removal is higher when the adsorption capacity is more. The adsorption capacity shows a poor positive correlation to electrical conductivity of the solution.

Removal efficiency

Different batch experiments were conducted based on the mixture appropriation earlier carried out. For the same set of mixture F^- Standard of 10 $mgl^{-1}$was prepared for each batch. 5 ml of sample was collected and analyzed. The average concentration of almost all the batches were around 0.5 (i.e.) the fluoride removal efficiency was 95 % but the efficiency of removal starts decreasing at batch 11 and 12. It is evident that after 5,946 min i.e. after 99 h and its further reduced to 90 % after 146 h. Hence for a known

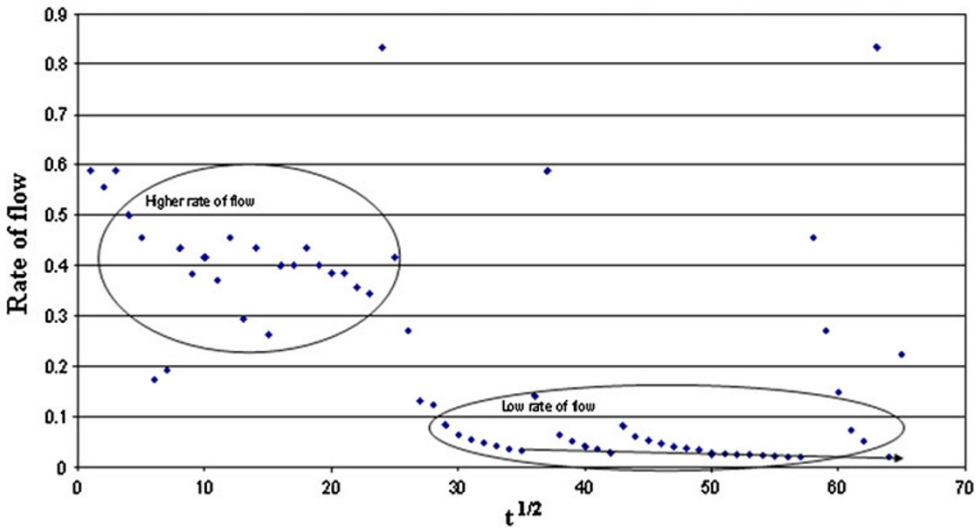

Fig. 2 Relation between rate of flow (mls^{-1}) and fluoride removal

volume of 946 cm^3 of materials the efficiency decreases from 99 h and as time progresses the pH become more acidic. In general, it was noted that the initial treated water collected from each batch had high pH and F^- concentration which tends to reduce during the reaction.

Fluoride removal capacity was determined by the Weber–Morris equation, the removal capacity varies during the experimental period. The rate of flow (q) ranges from 0.04 to 0.36, but the initial readings of each batch may even reach zero. The decrease of q starts from 4,489 min, until then the value almost remains constant. Plot shows the plot of rate of flow (q) vs. $t^{1/2}$ (Fig. 2). It was observed that the plots are linear over the whole time period and the plots exhibit a plateau, indicating that the external surface adsorption is dominant at the initial stage and stage of intra-particle diffusion is attained and continued up to 4,489 min (half of the experimental period) after which the equilibrium was attained. The anions are slowly transported via intra-particle diffusion into the pores of the adsorbent and finally retained in the particles. Also it was observed that the initial linear portion of the curve does not pass through the origin and later stage of fluoride adsorption does not obey Weber–Morris equation, which indicates that mechanism of fluoride adsorption is rather complex process and the intra-particle diffusion is not the only rate-limiting step (Thakrea et al. 2010). In general the removal capacity reduces from the initial time period its also interesting to note that at the beginning of each batch the removal capacity is lesser. This may be due to high rate of flow and lesser residence time for the fluoride to get adsorbed on to the material.

Rate of flow

It is observed that at a lower flow rate fluoride removal was efficient, at least in the initial stage of process, which may be due to the adequate contact time between adsorbent and adsorbate in solution. However, the extent of fluoride removal decreases with gradual occupancy of active sites of adsorbent. The rate of flow of the water through the medium is higher during the initial time periods with no definite trend and it is lesser in the last few batches. Figure 2 shows that there is a considerable decrease of pH and increase of HCO_3 concentration at the end of the experiment. At higher flow rate, fluoride removal capacity decreases and break-through becomes steeper and fluoride removal capacity is lesser due to shorter residence time of solute in the column, because of which, fluoride solution elutes the column before fluoride adsorption equilibrium occurs.

Regeneration studies

The reusability of the adsorbent was studied in order to check the residual fluoride uptake capacity. The reusability experiment was carried out by repeating the adsorption experiment on used and dried sample mixture under similar condition. The sediments after the experiment were washed with distilled water then dried in atmospheric conditions. Later the above experimental set up was repeated by the regenerated sediments.

The regenerated red soil to sand 4:1 was taken in the column and the experiment was repeated by passing 10 $mgl^{-1}$of fluoride standard solution. Initial 10 mgl^{-1} of F^- was passed through the column the F^- value reduced from 10 to 2.5 mgl^{-1} with a rate of removal of 0.007 at 314 min and further the rate of removal decreased to 0.003 at 1,410 min. In the 2:2 the rate of removal was 0.072 till 127 min and it got decreased to 0.028 and 0.035 at 296 and 328 min, respectively. It is interesting to note that the F^- concentration decreases at varying rate and increases after 21 h of the experiment in the regenerated soil.

Conclusions

The treatment of fluoride rich waters by using natural materials shows that there is a significant variation in FTIR spectrum before and after treatment. The variation is noted in the OH region of the spectrum, indicating adsorption and variation in bonding strength. The sites with Fe-OH and Al–OH bonds present in the red soil plays a main role in the controlling the efficiency of fluoride removal. Fluoride removal is effective in near neutral conditions. The competitiveness of the OH^- and F^- ions can be attributed to the change in pH of the solution. The effective removal of fluoride is maintained for a longer period and decreases with time after the occupation of the active sites. Though the rate of flow is higher at the initial stages the removal was effective due to the availability of more active sites. Subsequently the rate of flow was lesser and still the removal was found to be effective due to the increase of the contact time between the adsorbent and the liquid. The regeneration of the medium after the experiment for about 9,213 min was attempted and found to be effective, this also helps in the field for daily backwash of the column after the treatment and help to regenerate itself. The results obtained indicate this as a possible method for the removal of Fluoride for an effective rural water supply scheme. Further due to its control over the rate of water flow, column experiments is proved to be an easy method for transferring the technology to the field. This method requires no power supply since water moves down by the gravitational force hence it becomes more cost effective and easy to handle by local community as a suitable green and clean technology for rural drinking water supply in Fluoride affected areas.

Acknowledgments The authors wish to express their thanks to Ministry of Environment and Forest (MoEn&F), India for providing the necessary financial support to carry out this study vide letter No.1-6/2007-CT Dated 07.10.2009.

References

Agarwal M, Rai K, Shrivastav R, Dass S (2003) Deflouridation of water using amended clay. J Clean Prod 11:439–444

Amof Z, Barioub B, Mamer N, Taky M, Nicolas S, Elmidaoui A (2001) Fluoride removal Corn brackish water by electrodialysis. Desalination 133:215–223

Amor Z, Malki S, Taky M, Barioub B, Mamer N, Elmidaoui A (1998) Optimization of fluoride removal from brackish water by electrodialysis. Desalinisation 120:263–271

Annouar S, Tahaikt M, Mountadar M, Soufiane A (2007) A fluoride removal for underground brackish water by adsorption on the natural chitosan and by electrodialysis. Desalination 212:37–45

APHA (1998) Standard method for the examination of the water and waste water. American Public Health Association, Washington D.C, p 1268

Ayoob S, Gupta AK (2007) Sorptive response profile of an adsorbent in the defluoridation of drinking water. Chem Eng J 133: 273–281

Ayoob S, Gupta AK (2008) Insights into isotherm making in the sorptive removal of fluoride from drinking water. J Hazard Mater 152:976–985

Ayoob S, Gupta AK (2009) Performance evaluation of alumina cement granules in removing fluoride from natural and synthetic waters. Chem Eng J 150:485–491

Ayoob S, Gupta AK, Bhakat B, Bhat VT (2008) Investigations on the kinetics and mechanisms of sorptive removal of fluoride from water using alumina cement granules. Chem Eng J 140:6–14

Bansiwal A, Thakre D, Labhshetwar N, Meshram S, Rayalu S (2009) Fluoride removal using lanthanum incorporated chitosan beads. Colloids Surf B: Biointerfaces 74:216–224

Bansiwal A, Pillewan P, Biniwale RB, Rayalu SS (2010) Copper oxide incorporated mesoporous alumina for defluoridation of drinking water. Microporous Mesoporous Mater 129:54–61

Biswas K, Gupta K, Ghosh UC (2009) Adsorption of fluoride by hydrous iron (III)–tin(IV) bimetal mixed oxide from the aqueous solutions. Chem Eng J 149:196–206

Bower CA, Hatcher JT (1967) Adsorption of fluoride by soils and minerals. Soil Sci 103:209–218

Chauhan VS, Dwivedi PK, Iyengar L (2007) Investigations on activated alumina based domestic defluoridation units. J Hazard Mater B139:103–107

Chidambaram S (2000) Hydrogeochemical studies of groundwater in Periyar district, Tamil Nadu, India. Unpublished Thesis, Department of Earth Sciences, Annamalai University, India, 293 p

Chidambaram S, Ramanathan AL, Vasudevan S (2003) Fluoride removal studies in water using natural materials. Water SA 29:339–344

Chou W-L (2010) Removal and adsorption characteristics of polyvinyl alcohol from aqueous solutions using electrocoagulation. J Hazard Mater 177:842–850

Chukin GD, Malevich VI (1977) Infrared spectra of silica. J Appl Spectrosc 26:294–301

Das N, Pattanaik P, Das R (2005) Defluoridation of drinking water using activated titanium rich bauxite. J Colloid Interface Sci 292:1–10

Della Ventura G, Mottana A, Parodi GC, Griffith WL (1996) FTIR spectroscopy in the OH-stretching region of monoclinic epidotes from Praborna (St. Marcel, Aosta Valley, Italy). Eur J Mineral 8:655–665

Denning JH, Hudson RF, Laughlin DR, Ross SD, Sparasci AM (1972) The vibrational spectra of some rare-earth pyrosilicates. Spectrochim Acta 28A:1787–1791

Dutta M, Ray T, Basu JK (2012) Batch adsorption of fluoride ions onto microwave assisted activated carbon derived from Acacia Auriculiformis scrap wood. Arch Appl Sci Res 4(1):536–550

Elazhar F, Tahaikt M, Achatei A, Elmidaoui F, Taky M, El Hannouni F, Laaziz I, Jarir S, El Amrani M, Elmidaoui A (2009) Economical evaluation of the fluoride removal by nanofiltration. Desalination 249:154–157

Erguna E, Tor A, Cengeloglu Y, Kocak I (2008) Electrodialytic removal of fluoride from water: effects of process parameters and accompanying anions. Sep Purif Technol 64:147–153

Essadki AH, Gourich B, Vial Ch, Delmas H, Bennajah M (2009) Defluoridation of drinking water by electrocoagulation/electroflotation in a stirred tank reactor with a comparative performance

to an external-loop airlift reactor. J Hazard Mater 168: 1325–1333
Gao S, Sun R, Wei Z, Zhao H, Li H, Hu F (2008) Size-dependent defluoridation properties of synthetic hydroxyapatite. J Fluor Chem 130:550–556
Gao S, Cui J, Wei Z (2009) Study on the fluoride adsorption of various apatite materials in aqueous solution. J Fluor Chem 130:1035–1041
Garmes H, Persin F, Sandeaux J, Pourcelly G, Mountadar M (2002) Defluoridation of groundwater by a hybrid process combining adsorption and Donnan dialysis. Desalination 145:287–291
Ghorai S, Pant KK (2005) Equilibrium, kinetics and breakthrough studies for adsorption of fluoride on activated alumina. Sep Purif Technol 42:265–271
Ghosh D, Medhi CR, Purkait MK (2008) Treatment of fluoride containing drinking water by electrocoagulation using monopolar and bipolar electrode connections. Chemosphere 73:1393–1400
Gupta VK, Ali I, Saini VK (2007) Defluoridation of waste waters using waste carbon slurry. Water Res 41:3307–3316
Hawthorne FC (1983) The crystal chemistry of amphiboles: a review. Can Mineral 21:173–480
Hichour M, Persin F, Sandeaux J, Gavach C (2000) Fluoride removal from waters by Donnan dialysis. Sep Purif Technol 18:1–11
Ho Y-S (2009) Comments on defluoridation of water using neodymium-modified chitosan. J Hazard Mater 172:515
Hua CY, Loa SL, Kuan WH (2003) Effects of co-existing anions on fluoride removal in electrocoagulation (EC) process using aluminum electrodes. Water Res 37:4513–4523
Hua CY, Loa SL, Kuan WH (2005) Effects of the molar ratio of hydroxide and fluoride to Al(III) on fluoride removal by coagulation and electrocoagulation. J Colloid Interface Sci 283:472–476
Kagne S, Jagtap S, Thakare D, Devotta S, Rayalu SS (2009) Bleaching powder: a versatile adsorbent for the removal of fluoride from aqueous solution. Desalination 243:22–31
Kamble S, Jagtap S, Labhsetwar N, Thakre D, Godfrey S, Devotta S, Rayalu SS (2007) Defluoridation of drinking water using chitin, chitosan and lanthanum modified chitosan. Chem Eng J 129:173–180
Karthikeyan M, Elango KP (2009) Removal of fluoride from water using aluminium containing compounds. J Environ Sci 21: 1513–1518
Karthikeyan M, Satheesh Kumar KK, Elango KP (2009) Conducting polymer/alumina composites as viable adsorbents for the removal of fluoride ions from aqueous solution. J Fluorine Chem 130:894–901
Kemer B, Ozdes D, Gundogdu A, Bulut VN, Duran C, Soylak M (2009) Removal of fluoride ions from aqueous solution by waste mud. J Hazard Mater 168:888–894
Kumar E, Bhatnagar A, Ji M, Jung W, Lee S-H, Kim S-J, Lee G, Song H, Choi J-C, Yang J-S, Jeon B-H (2009) Defluoridation from aqueous solutions by granular ferric hydroxide (GFH). Water Res 43:490–498
Lahnida S, Tahaikta M, Elarouia K, Idrissia I, Hafsi M, Laaziz I, Amora Z, Tiyala F, Elmidaoui A (2008) Economic evaluation of fluoride removal by electrodialysis. Desalination 230:213–219
Lazarev AN (1972) Vibrational Spectra and Structure of Silicates. Plenum Press, New York
Lv L, Heb J, Wei M, Evans DG, Zhou Z (2007) Treatment of high fluoride concentration water by MgAl-CO3 layered double hydroxides: kinetic and equilibrium studies. Water Res 41: 1534–1542
Ma Yue, Wang S-G, Fan M, Xin W-X, Gao BY (2009) Characteristics and defluoridation performance of granular activated carbons coated with manganese oxides. J Hazard Mater 168: 1140–1146
Makreski P, Jovanovski G, Stojanceska S (2005) Minerals from Macedonia XIII: vibration spectra of some commonly appearing nesosilicate minerals. J Mol Struct 744–747:79–92
Makreski P, Jovanovski G, Kaitner B, Gajovic A, Biljan T (2007) Minerals from Macedonia XVIII. Vibrational spectra of some sorosilicates. Vib Spectrosc 44:162–167
Malakootian M, Moosazadeh M, Yousefi N, Fatehizadeh A (2011) Fluoride removal from aqueous solution by pumice: case study on Kuhbonan water. Afric J Environ Sci Technol 5(4):299–306
Malay DK, Salim AJ (2011) Comparative study of batch adsorption of fluoride using commercial and natural adsorbent. Res J Chem Sci 1(7):68–75
Mameri N, Lounici H, Belhocine D, Grib H, Piron DL, Yahiat Y (2001) Defluoridation of Sahara water by small plant electrocoagulation using bipolar aluminium electrodes. Sep Purif Technol 24:113–119
Mandal S, Mayadevi S (2009) Defluoridation of water using as-synthesized Zn/Al/Cl anionic clay adsorbent: equilibrium and regeneration studies. J Hazard Mater 167:873–878
Meenakshi M, Maheshwari RC (2006) Fluoride in drinking water and its removal. J Hazard Mater B137:456–463
Mekonen A, Kumar P, Kumar A (2001) Integrated biological and physiochemical treatment process for nitrate and fluoride Removal. Water Res 35(13):3127–3136. doi:S0043-1354(01)00019-7
Mjengera H, Mkongo G (2003) Appropriate deflouridation technology for use in flourotic areas in Tanzania. Phys Chem Earth 28:1097–1104
Mohapatra M, Anand S, Mishra BK, Giles DE, Singh P (2009) Review of fluoride removal from drinking water. J Environ Manage 91:67–77
Mustard JF (1992) Chemical analysis of actinolite from reflectance spectra. Am Miner 77:345–358
Nicolas S, Guihard L, Marchand A, Bariou B, Amrane A, Ali A, Nabil N, El Midaoui A (2010) Defluoridation of brackish northern Sahara. Activity product calculations in order to optimize pretreatment before reverse osmosis. Desalination 256:9–15
Nigussie W, Zewge F, Chandravanshi BS (2007) Removal of excess fluoride from water using waste residue from alum manufacturing process. J Hazard Mater 147:954–963
Ramos RL, Ovalle-Turrubiartes J, Sanchez-Castillo MA (1999) Adsorption of fluoride from aqueous solution on aluminum impregnated carbon. Carbon 37:609–617
Rao M, Subba Rao VB, Prasanthi M, Muppa Ravi V (2009) Characterization and defluoridation studies of activated dolichos. Lab carbon 2:525–530
Rutstein MS, White WB (1971) Vibrational spectra of high-calcium pyroxenes and pyroxenoids. Am Miner 56:877–887
Sairam Sundaram C, Meenakshi S (2009) Fluoride sorption using organic–inorganic hybrid type ion exchangers. J Colloid Interface Sci 333:58–62
Sairam Sundaram C, Viswanathan N, Meenakshi S (2008a) Uptake of fluoride by nano-hydroxyapatite/chitosan, a bioinorganic composite. Bioresour Technol 99:8226–8230
Sairam Sundaram C, Viswanathan N, Meenakshi S (2008b) Defluoridation chemistry of synthetic hydroxyapatite at nano scale: equilibrium and kinetic studies. J Hazard Mater 155:206–215
Sajidu S, Kayira C, Masamba W, Mwatseteza J (2012) Defluoridation of groundwater using raw bauxite: rural domestic defluoridation technology. Environ Nat Resour Res 2(3):1–9
Sarkar M, Banerjee A, Pramanick PP, Sarkar AR (2006) Use of laterite for the removal of fluoride from contaminated drinking water. J Colloid Interface Sci 302:432–441
Singh IB, Prasad M, Amritphale SS (2004) Development of defluoridation technology for its easy adaptation in rural areas. J Rural Technol 1(4):163–167

Sivasankara V, Ramachandramoorthy T, Chandramohan A (2010) Fluoride removal from water using activated and MnO2-coated Tamarind Fruit (Tamarindus indica) shell: batch and column studies. J Hazard Mater 177:719–729

Skogby H, Annersten H (1985) Temperature dependent Mg-Fecation distribution in actinolite-tremolite. Neues Jahrbuch ftir Mineralogie Monatshefte 13:193–203

Solangi IB, Shahabuddin Memon S, Bhanger MI (2009) Removal of fluoride from aqueous environment by modified Amberlite resin. J Hazard Mater 171:815–819

Sterns RGJ (1974) The common chain ribbon and ring silicates. In: Farmer VC (ed) Infrared Spectra of Minerals. Mineralogical Society, London, p 305p

Stubican V, Roy R (1961a) Isomorphous substitution and infrared spectra of the Layer lattice silicates. Am Mineral 46:32–51

Stubican V, Roy R (1961b) A new approach to assignment of infrared absorption bands in layer-structure silicates. Zeil Krist 115:200–214

Tahaikt M, Achary I, Sahli MAM, Amor Z, Taky M, Alami A, Boughriba A, Hafsi M, Elmidaouia A (2004) Defluoridation of Moroccan ground water by electro dialysis continuous operation. Desalinisation 167:357

Tahaikt M, Acharya I, Sahli MAM, Amor Z, Taky M, Alami A, Boughriba A, Hafsi M, Elmidaouia A (2006) Defluoridation of Moroccan groundwater by electrodialysis: continuous operation. Desalination 189:215–220

Tahaikta M, Ait Haddou A, El Habbania R, Amor Elhannouni F, Taky M, Kharif M, Boughrib A, Hafsi M, Elmidaoui A (2008) Comparison of the performances of three commercial membranes in fluoride removal by nanofiltration, continuous operations. Desalination 225:209–219

Tang Y, Guan X, Wang J, Gao N, McPhail MR, Chusuei CC (2009) Fluoride adsorption onto granular ferric hydroxide: Effects of ionic strength, pH, surface loading, and major co-existing anions. J Hazard Mater 171:774–779

Thakrea D, Jagtapa S, Sakharea N, Labhsetwara N, Meshramb S, Rayalua S (2010) Chitosan based mesoporous Ti–Al binary metal oxide supported beads for defluoridation of water. Chem Eng J 158:315–324

Togarepi E, Mahamadi C, Mangombe A (2012) Deflouridation of water using physico-chemically treated sand as a low-cost adsorbent: an equilibrium study. Afri J Environ Sci Technol 6(3):176–181

Tripathy SS, Bersillon J-L, Gopal K (2006) Removal of fluoride from drinking water by adsorption onto alum-impregnated activated alumina. Sep Purif Technol 50:310–317

Viswanathan N, Meenakshi S (2008) Enhanced fluoride sorption using La (III) incorporated carboxylated chitosan beads. J Colloid Interface Sci 322:375–383

Viswanathan N, Meenakshi S (2009a) Role of metal ion incorporation in ion exchange resin on the selectivity of fluoride. J Hazard Mater 162:920–930

Viswanathan N, Meenakshi S (2009b) Synthesis of Zr (IV) entrapped chitosan polymeric matrix for selective fluoride sorption. Colloids Surf, B 72:88–93

Viswanathan N, Sairam Sundaram C, Meenakshi S (2009a) Development of multifunctional chitosan beads for fluoride removal. J Hazard Mater 167:325–331

Viswanathan N, Sairam Sundaram C, Meenakshi S (2009b) Removal of fluoride from aqueous solution using protonated chitosan beads. J Hazard Mater 161:423–430

Viswanathan N, Sairam Sundaram C, Meenakshi S (2009c) Sorption behaviour of fluoride on carboxylated cross-linked chitosan beads. Colloids Surf, B 68:48–54

Wajima T, Umeta Y, Narita S, Sugawara K (2009) Adsorption behavior of fluoride ions using a titanium hydroxide-derived adsorbent. Desalination 249:323–330

Wang A, Han J, Guo L, Yu J, Zeng P (1994) Database of standard Raman spectra of minerals and related inorganic crystals. Appl Spectrosc 48:959–968

Wilkens RWT (1970) Iron-magnesium distribution in the tremolite actinolite series. Am Mineral 5(5):1993–1998

Wisniewski J, Rozanska A, Winnick T (2005) Removal of troublesome anions from water by means of Donnan dialysis. Desalination 182:339–346

Yadav AK, Kaushik CP, Haritash AK, Kansal A, Rani N (2006) Defluoridation of groundwater using brick powder as an adsorbent. J Hazard Mater B128:289–293

Yao R, Meng F, Zhang L, Ma D, Wang M (2008) Defluoridation of water using neodymium-modified chitosan. J Hazard Mater 165:454–460

Zhu J, Zhao H, Jinren N (2007) Fluoride distribution in electrocoagulation defluoridation process. Sep Purif Technol 56:184–191